


# Study on the Effect of Lesion Volume and Focal Temperature Caused by HIFU Combined with Different Concentrations and Volumes of Ethanol on Porcine Liver

Hu Dong (PhD)<sup>1\*</sup>, Jiwen Hu (PhD)<sup>2</sup>, Xiao Zou (PhD)<sup>3</sup>, Wei Chen (PhD)<sup>4</sup>

## ABSTRACT

**Background:** High-intensity Focused Ultrasound (HIFU) is a rapidly developing non-invasive treatment method for tumors in recent years.

**Objective:** The present study aimed to investigate the lesion and temperature effects of HIFU combined with different concentrations and volumes of ethanol on porcine liver.

**Material and Methods:** In this experimental study, different concentrations and volumes of ethanol were injected into the focal area of porcine liver using B-mode ultrasound, and the focal temperature was monitored using a k-type needle thermocouple. The peak negative pressure and sound intensity at the focal point of porcine liver were calculated by Khokhlov-Zabolotskaya-Kuznetsov (KZK) equation. Further, the presence of cavitation effects within porcine liver was further determined by ultrasound hyperechoic. The differences in lesion volume and temperature, caused by different concentrations and volumes of ethanol on porcine liver, were measured.

**Results:** HIFU irradiation combined with ethanol injection caused greater lesion volume and higher focal temperature in porcine liver. At the same HIFU irradiation power, an increase in the volume of ethanol resulted in an increase in lesion volume and focal temperature. At a fixed volume of ethanol injected and HIFU irradiation power, higher ethanol concentrations resulted in higher lesion volumes and focal temperature.

**Conclusion:** The combination of HIFU and ethanol synergistically affects the lesion of porcine liver, manifested as the larger the ethanol concentration and volume, the larger the lesion volume and the higher the focal temperature.

**Citation:** Dong H, Hu J, Zou X, Chen W. Study on the Effect of Lesion Volume and Focal Temperature Caused by HIFU Combined with Different Concentrations and Volumes of Ethanol on Porcine Liver. *J Biomed Phys Eng.* 2025;15(1):15-26. doi: 10.31661/jbpe.v0i0.2403-1737.

## Keywords

High-Intensity Focused Ultrasound; Negative Pressure; Ethanol; Temperature

## Introduction

High-intensity Focused Ultrasound (HIFU) mainly uses the transmissibility and energy deposition of ultrasound to gather the lower-energy ultrasound occurring *in vitro* to deep tumor foci *in vivo*. Through the transient high-temperature (more than 60 °C), cavitation, and mechanical effects produced by high-energy ultrasound in the focusing area, proteins are denaturalized, as well as irreversible

<sup>1</sup>School of Information Science and Engineering, Changsha Normal University, Changsha 410100, China

<sup>2</sup>School of Mathematics and Science, Nanhua University, Hengyang, 421001, China

<sup>3</sup>School of Physics and Electronics, Hunan Normal University, Changsha 410081, China

<sup>4</sup>School of Electronic Information and Electrical Engineering, Changsha University, Changsha, 410022, China

\*Corresponding author:

Hu Dong

School of Information Science and Engineering, Changsha Normal University, Changsha 410100, China

E-mail: weijundong203@outlook.com

Received: 18 March 2024

Accepted: 20 June 2024

damage of the cells, and coagulative necrosis, which can further kill the tumor cells [1-4]. The tissue passed by the ultrasound beam and the tissue outside the target area will not be damaged, which has the advantages of safety and reliability, accurate positioning, non-traumatic, fast recovery after treatment, and no drug side effects.

During the propagation process of ultrasound, energy attenuation occurs due to the absorption, reflection, and scattering of biological tissue, and the degree of attenuation becomes more and more severe with the increase of propagation distance [5-6]. At the same time, due to the small volume of the basic ablation point of HIFU, the point superposition mode is usually used during treatment, which leads to the problems of long irradiation time and low treatment efficiency in HIFU treatment. Therefore, how to improve the treatment efficiency of HIFU and shorten the treatment time has become a hot research topic. Related studies have shown that in the process of HIFU treatment, the efficiency of HIFU treatment for tumors can be improved by adding certain substances to alter the acoustic properties or environment of the tissue, increase the deposition of HIFU ultrasound energy, and reduce the threshold of cavitation effect.

Some studies have experimentally confirmed that ethanol can lower the threshold of inertial cavitation in tissue [7-10]. Ethanol is usually used as a deformer because its surface tension at 20 °C is 22.27 mN/m, which is much lower than that of 71.97 mN/m in water, and its air solubility is 10-20 times higher than that of water. Therefore, the cavitation threshold in ethanol should be lower than that in water because of the lower surface tension and higher air solubility in ethanol [11]. Percutaneous Ethanol Injection (PEI) is a major chemical ablation method. In the 1980 s, it was frequently used for non-surgical treatment of cancer. PEI is based on the fact that the interaction of ethanol with living tissue leads to cellular dehydration, protein denaturation, and

thrombosis of small blood vessels [12], which is a safe, inexpensive, and easy-to-implement technique. There are more studies on injecting ethanol into HIFU for tumor treatment. Chen et al. treated bovine liver with 2 ml of pure (99.5%) ethanol and irradiated it with 0.825 MHz HIFU to study its cavitation activity and temperature rise. The results of the study showed that the treatment of tissue models and bovine liver samples with ethanol decreased the threshold power of its inertial cavitation [7]. Hoang et al. investigated the combined effect of ethanol and HIFU on porcine liver tissue by injecting 0.2 mL of ethanol at 95% concentration into porcine liver tissue and irradiating them with HIFU. The results showed that sequential application of ethanol and HIFU significantly enhanced the destruction of liver tumors [8]. Yang et al. combined HIFU with anhydrous ethanol for the treatment of uterine fibroids, and the results of their study found that compared to the treatment of uterine fibroids with HIFU alone, HIFU combined with anhydrous ethanol produced a larger volume of damage, less treatment time and required a lower therapeutic dose, and significantly reduced the patient's common pain and side effects [9]. Lang et al. used HIFU in combination with a 95% concentration of ethanol for the treatment of benign thyroid nodules, and HIFU combined with ethanol was more effective in the treatment of benign thyroid nodules compared with HIFU ablation alone [10].

However, it is unclear whether injecting different volumes and concentrations of ethanol into biological tissue will produce similar therapeutic effects as mentioned above. Therefore, this article analyzes the effects of injecting different concentrations and volumes of ethanol into isolated porcine liver tissue and combining them with HIFU of different powers for irradiation, on the volume of lesion and focal temperature of porcine liver tissue. The aim is to explore the effect and influence of different concentrations and volumes of

ethanol on HIFU ablation.

## Material and Methods

### Experiment equipment and materials

In this experimental study, porcine liver tissue freshly obtained from the abattoir was tested by immersing it in a 0.9% saline solution. In order to remove oxygen from the water, polyvidone and pure ethanol were mixed in a 1:3.5 ratio. They were then mixed with water in a ratio of 1:22 and poured into a water tank. Porcine liver tissue was placed in the water tank directly below the HIFU source (PROM2008, Shenzhen, CN), while the porcine liver was fixed on the sample holder, and ultrasound transmission distance in water was 8 cm. In combination with an ultrasound probe, different volumes of 20% low-concentration ethanol and 95% high-concentration ethanol were injected into the focal position of the porcine liver with a syringe before HIFU irradiation of the porcine liver, respectively. A k-type needle thermocouple (DT-3891G, Shenzhen, CN) with a diameter of 0.5 mm was inserted near the focal area, with the thermocouple tip at a distance of about 2 mm from the focal distance for more accurate monitoring of the temperature at the focal point of the porcine liver. The bottom of the tank was filled with acoustic rubber to absorb ultrasound waves, and a computer-controlled three-dimensional moving platform was used to adjust the position of the HIFU transducer. A self-focusing ultrasound transducer was used as the HIFU source in the experiments. Its concave spherical surface and circular aperture at the top allowed the passage of a B-mode ultrasound probe. The center frequency of the self-focusing transducer was 1.2 MHz, the geometric focal length was 10 cm, the diameter of the outer aperture of the transducer was 9.2 cm, and the diameter of the inner aperture was 4.4 cm. The duration of each HIFU irradiation was 5 s. The experimental setup for cavitation detection and temperature measurement is shown in

Figure 1.

### Principle and method

It is well known that the Khokhlov-Zabolotskaya-Kuznetsov (KZK) equation is only applicable to focused ultrasound transducers with a semi-aperture angle of less than 16 degrees, but the KZK equation was used to model transducers with low f-numbers and achieved good agreement with actual measurements [13]. Therefore, the KZK equation was utilized to simulate the acoustic field at the focal point of the porcine liver. KZK equation is given below [14-16]:

$$\frac{\partial}{\partial z'} \left( -\frac{c_0}{2} \frac{\partial p}{\partial z'} + \frac{\partial p}{\partial t'} \right) = \frac{c_0}{2} \nabla_{\perp}^2 p + \frac{\delta}{2c_0^3} \frac{\partial^3 p}{\partial t'^3} + \frac{\beta}{2\rho_0 c_0^3} \frac{\partial^2 p^2}{\partial t'^2} \quad (1)$$

where,  $p$  is the acoustic pressure,  $\tau=t-z/c_0$  is the delay time,  $c_0$  is the speed of sound,  $\delta$  is the

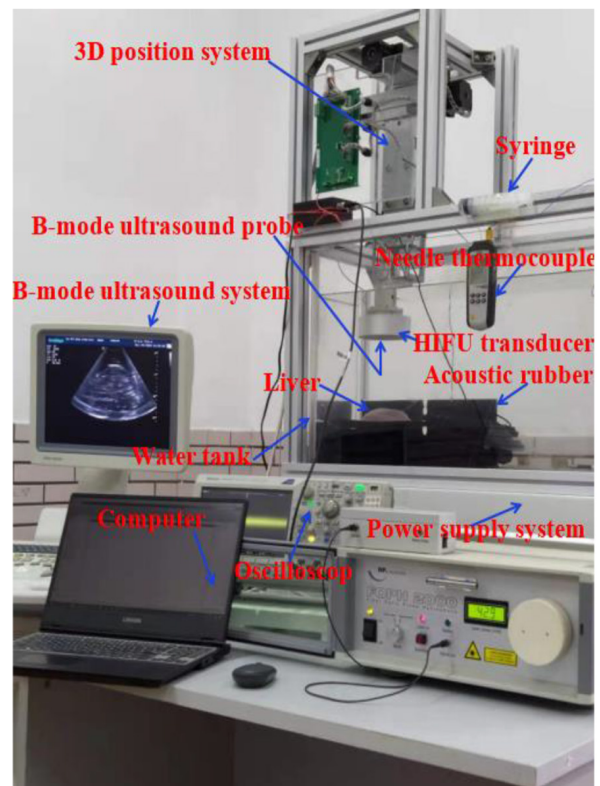


**Figure 1:** The experimental setup for cavitation detection and temperature measurement

acoustic diffusivity of the biological tissue,  $\beta$  is the nonlinear coefficient of the tissue,  $\rho_0$  is the density of the medium,  $\nabla_{\perp}$  is the Laplace operator, which is denoted as  $\nabla_{\perp} = \partial^2 / \partial x^2 + \partial^2 / \partial y^2$  in the right-angled coordinate system and as  $\nabla_{\perp} = \frac{1}{r} \frac{\partial}{\partial r} \left( r \frac{\partial}{\partial r} \right) + \frac{1}{r^2} \frac{\partial^2}{\partial \theta^2}$  in the cylindrical coordinate system. When the frequency of the acoustic wave is when  $f_0$ , the acoustic absorption coefficient of the medium is  $\alpha_0 = w^2 \delta / (2c_0^2)$ . The sound absorption coefficient  $\alpha$  is related to the frequency  $f$  as follows [17]:

$$\alpha(f) = \alpha_0 (f / f_0)^{\mu} \quad (2)$$

In the Frequency domain, the sound pressure is represented as a Fourier series expansion [18]:

$$p = \sum_{n=-\infty}^{\infty} C_n \exp(jn\tau) \quad (3)$$

$C_n$  is the complex coefficient of the nth-order harmonic.

$$\frac{dC_n}{dz} = -\frac{in\beta}{2c^3\rho} \sum_{k=-\infty}^{\infty} C_k C_{n-k} + i \frac{c}{4\pi f_0 n} \nabla_{\perp} C_n - \left( \alpha(nf_0) - i \frac{2nf_0}{(\eta-1)\pi f_*} (\alpha(nf_0) - \alpha(f_0)) \right) C_n \quad (4)$$

In sound field calculations, the sound intensity at the HIFU focal point can be represented by the amplitude values of each harmonic wave of sound pressure [19]:

$$I = \frac{\langle p^2 \rangle}{\rho c} = 2 \sum_{n=1}^{\infty} |C_n|^2 / \rho c \quad (5)$$

In the numerical simulation, the Finite Difference Time Domain (FDTD) method was used to solve the acoustic field model emitted by a unitary self-focusing ultrasonic transducer [20-21].

A two-layer nonlinear acoustic propagation model was constructed with the KZK equation for simulation calculation. The acoustic parameters used for the simulation calculation are shown in Table 1.

**Table 1:** Acoustic parameters of water and liver [22-24]

Material	$\rho_0$ (kg/m <sup>3</sup> )	$c_0$ (m/s)	$\alpha$ (dB/m)	B/A
Water	1000	1482	0.217	5.0
Liver	1036	1590	58	6.6

## Results

Five different HIFU power ( $p'$ ), 105 W, 115 W, 125 W, 135 W, and 145 W, were used to irradiate porcine liver tissue (ignoring cavitation effects). The spatial grid parameters used for sound field simulation were  $dz=0.063$  mm and  $dr=0.047$  mm. Using MATLAB R2018b (MathWorks, Natick, Massachusetts, United States) software to simulate and calculate the sound field in porcine liver tissue, the nonlinear harmonic order was 64, and the time step of the sound field was  $3.7 \times 10^{-9}$  seconds.

The sound field waveforms obtained from the simulation using the KZK equation are shown in Figure 2. Where,  $p_1$  and  $p_2$  were sound pressure, and  $I$  was the acoustic intensity.  $V_{rms}$  was the root mean square voltage measured after the HIFU amplifier, and  $P_{-}$  was the peak negative pressure in the focus of porcine liver.

The higher the HIFU irradiation power causes the greater the sound pressure, peak negative pressure, and axial focus position sound intensity at the focal point (Figure 2).

The simulated sound field parameters for five different HIFU power-irradiated porcine liver tissues are shown in Table 2.

From the simulation results in Table 2, it can be seen that the higher the HIFU power, the greater the corresponding focal position sound intensity,  $V_{rms}$ , and peak negative pressure.

Although some previous studies have found thermal effects related to cavitation, the thermal effects caused by bubble activity deserve close attention. Cavitation bubbles often increase the local attenuation coefficient of ultrasound, and the stronger acoustic



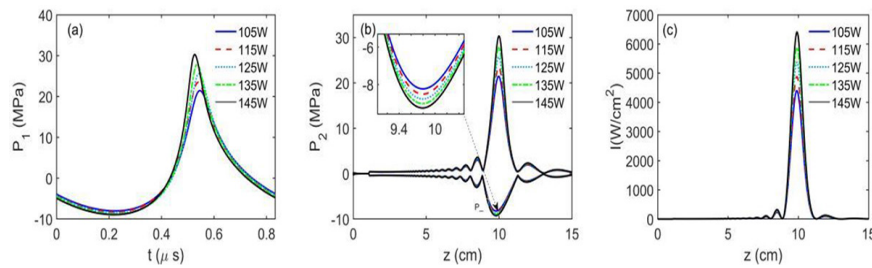


**Figure 2:** (a) Pressure waveform at the focus; (b) Peak positive and negative pressure; (c) Acoustic intensity

**Table 2:** Simulation parameters of the sound field under different HIFU power

$p'(W)$	$I(W/cm^2)$	$V_{rms}(V)$	$P_(MPa)$
105	4373	51.2	8.2
115	4878	53.6	8.5
125	5374	55.9	8.8
135	5883	58.1	9.0
145	6408	60.2	9.3

attenuation that occurs in the presence of cavitation bubbles can enhance heating related to ultrasound absorption [25]. The negative pressure caused by HIFU sound waves is large enough to cause cavitation, and higher pressure increases the probability of cavitation occurring [26]. Bull et al. found that when the pressure threshold exceeded 1.86 MPa, 100% cavitation occurred in *ex vivo* bovine liver [27]. McLaughlan et al. reported that at 1.69 MHz, the cavitation threshold of *ex vivo* bovine liver was about 2.0 MPa, which mainly depended on the relative content (or concentration) of water and lipids in the tissue [28]. Li et al. found that cavitation occurs when the negative pressure at the focal region of the detached bovine liver exceeds 5 MPa [29]. The peak negative pressure generated under different HIFU power irradiation reaches at least 8.2 MPa, which far exceeds the reported pressure threshold for cavitation in the liver, showing cavitation may

occur in the focal area of porcine liver tissue when HIFU is irradiated.

In addition, Rabkin et al. demonstrated that when the sound intensity was 850 W/cm<sup>2</sup>, the temperature rapidly increased after cavitation occurred, and cavitation occurred within the rabbit thigh muscles at 0.32 seconds [30]. In this experiment, when the irradiation power of the HIFU transducer is 105 W, the corresponding sound intensity is 4373 W/cm<sup>2</sup>, which is much greater than the sound intensity of 850W/cm<sup>2</sup>. Therefore, it is inferred that cavitation effect may occur in porcine liver tissue after 6 seconds of HIFU irradiation at 105 W power. Therefore, we could not neglect the effect of cavitation.

The presence of cavitation is thought to be responsible for the appearance of hyperechoic areas in ultrasound images [31]. Since the 1990s, there has been increasing evidence that HIFU-induced acoustic cavitation can be monitored in real time by the formation of “bright spots” in the hyperechoic region of the ultrasound image during HIFU treatment [32-35]. Hynynen et al. pointed out that in the experiment of HIFU *in vivo* ablation of dog leg muscles, after the first ultrasound pulse is emitted, the Passive Cavitation Detector (PCD) inertial cavitation signal can be detected simultaneously with the appearance of the B-ultrasound bright area [32]. Vaezy et al. claimed that during real-time ultrasound imaging observations, bright spots were found escaping from the HIFU focal point into the

vascular system of liver tissue in the body [33]. In addition, researchers also found a high degree of correlation between the appearance of bright areas and the generation of cavitation bubbles [34-35]. Therefore, the present study demonstrates the occurrence of cavitation in porcine liver irradiated with HIFU through the bright area of ultrasound, and further explores the effects of cavitation caused by injection of different concentrations and lesion volumes of ethanol on the volume and focal temperature of porcine liver.

Under the guidance of B-mode ultrasound, different concentrations and volumes of ethanol were injected into the focal points of porcine liver tissue and irradiated with HIFU. A hyperechoic “bright spot” was obtained as shown in Figure 3.

Figure 3 shows the “bright spots” of hyperechoic areas produced in porcine liver tissue

by 105 W HIFU irradiation. As the volume of the injected ethanol gradually increased, the produced hypoechoic zone also gradually expanded, as shown in Figure 3(a) to (c), or Figure 3(d) to (f). For the same volume of ethanol injected, the hyperechoic zone produced by 95% ethanol was significantly larger than the hyperechoic zone produced by 20% ethanol, as shown in Figure 3 (a) and (d).

Figure 4 shows the cross-sectional images of thermal lesions caused by injecting different volumes of 20% and 95% ethanol into porcine liver tissue under 105 W HIFU irradiation. Among them, Figure 4(a) and (e) show the thermal lesion cross-sectional area generated by irradiating porcine liver tissue using only 105 W HIFU. Figure 4 (b)~(d) show the thermal lesion cross-sectional area generated by injecting different volumes of 20% concentration ethanol into porcine liver tissue

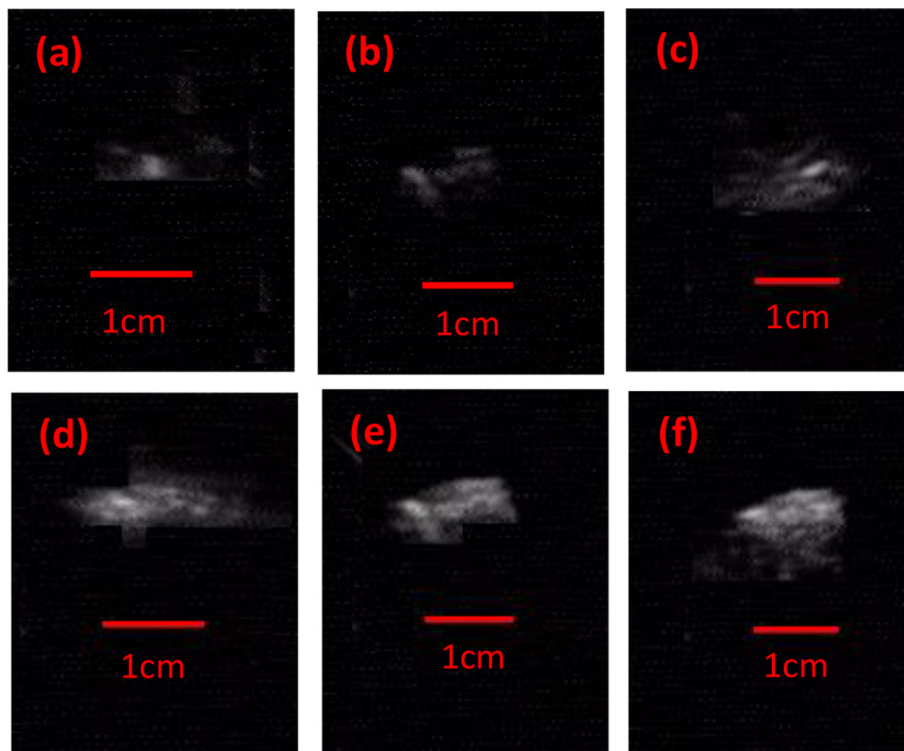


**Figure 3:** Hyperechoic samples of B-mode images of porcine liver caused by HIFU under different ethanol concentrations and volumes ((a) 105 W+0.2 ml 20% ethanol, (b) 105 W+0.6 ml 20% ethanol, (c) 105 W+1.0 ml 20% ethanol, (d) 105 W+ 0.2 ml 95% ethanol, (e) 105 W+0.6 ml 95% ethanol, (f) 105 W+1.0 ml 95% ethanol)

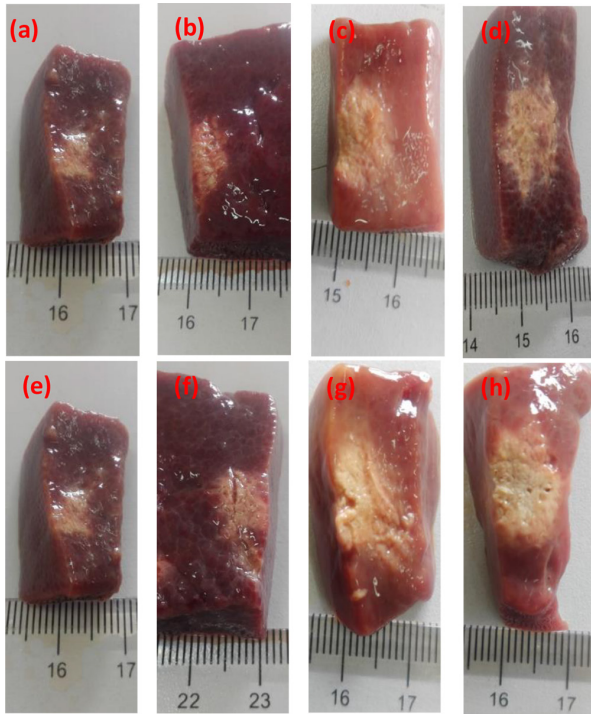


**Figure 4:** Comparison of thermal lesion area caused by HIFU under different ethanol concentrations and volumes ((a) 105 W HIFU only, (b) 105 W+0.2 ml 20% ethanol, (c) 105 W+0.6 ml 20% ethanol, (d) 105 W+1.0 ml 20% ethanol, (e) 105 W HIFU only, (f) 105 W+0.2 ml 95% ethanol, (g) 105 W+0.4 ml 95% ethanol, (h) 105 W+0.6 ml 95% ethanol).

under 105 W HIFU irradiation. Figure 4 (f)~(h) show the cross-sectional area of thermal lesion generated by injecting different volumes of 95% ethanol into porcine liver tissue under 105 W HIFU irradiation. Under the same HIFU irradiation power, as the volume of ethanol injected into porcine liver tissue gradually increased, the resulting lesion area showed a trend of increasing from small to large. At the same HIFU power and ethanol volume, the lesion area caused by a 95% concentration of ethanol was greater than that caused by a 20% concentration of ethanol.

After the HIFU irradiation experiment was completed, the liver tissue was dissected in the midsagittal plane perpendicular to the HIFU beam direction to measure the height H and length L of the thermal lesion volume generated in the porcine liver. The liver tissue is horizontally cut to measure the width W of the lesion. The lesion volume was calculated using the ellipsoidal volume formula [36].

$$V = \frac{\pi LWH}{6} \tag{6}$$

When the HIFU sound intensity gradually increased, the volume of lesion generated gradually increased in porcine liver tissue (Figure 5 (a)), and the focal temperature also

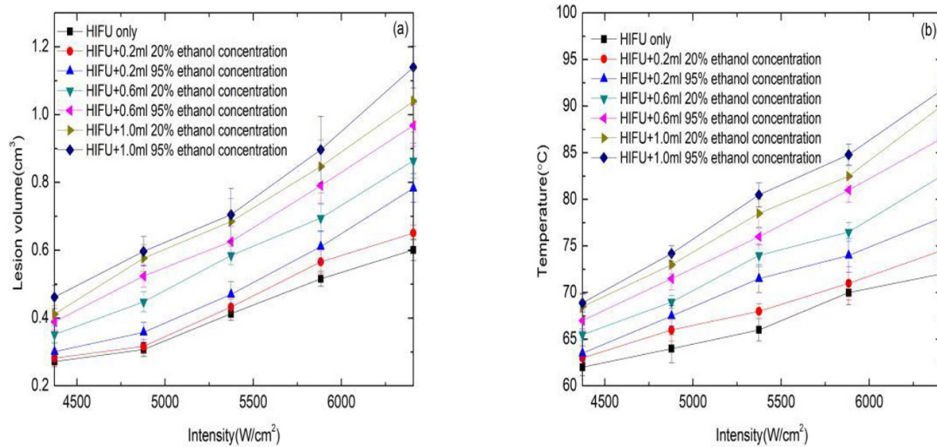


**Figure 5:** Different HIFU irradiation intensities, ethanol concentrations, and volumes to (a) Comparison of the volume of thermal lesions in porcine liver; (b) Comparison of peak focal temperature in porcine liver

gradually increased (Figure 5 (b)). Under the same sound intensity and injection volume of ethanol, the lesion volume and focal temperature produced by a 95% concentration of ethanol should be greater than those produced by a 20% concentration of ethanol. In addition, under the same sound intensity conditions, the use of only HIFU irradiation on porcine liver tissue resulted in a larger volume of lesions compared to HIFU irradiation and injecting ethanol into its focal region.

Similarly, using HIFU irradiation alone on porcine liver tissue resulted in a lower focal temperature compared to the combination of HIFU and ethanol injection at the focal region. Furthermore, under constant sound intensity and ethanol concentration, increasing the injected ethanol volume led to a gradual increase in both the focal temperature and the lesion volume caused by HIFU irradiation.

## Discussion

The combination of HIFU and ultrasound-guided injection of ethanol into porcine liver tissue not only combined the advantages of HIFU and ethanol, but also compensated for their respective shortcomings. On the one hand, HIFU concentrated ultrasound energy in a specific focal area, where the temperature can rapidly rise to 65 °C or even higher due to the thermal and cavitation effects of HIFU [37]. On the other hand, ethanol can reduce the threshold power of initial inertial cavitation, which in turn can cause a rapid increase in the temperature of the ethanol-treated sample at lower HIFU power. Therefore, injecting an appropriate amount of ethanol into porcine liver tissue can enhance the therapeutic effect of HIFU.

The research results indicated that ethanol can reduce the inertial cavitation threshold in liver tissue, and the combination of HIFU and ethanol had a synergistic effect on liver tissue lesions. Under the same irradiation conditions, the lesion volume produced by HIFU combined with ethanol in porcine liver tissue

was significantly greater than that produced by HIFU alone, indicating that HIFU combined with ethanol had a higher therapeutic efficiency. The lesion volume and focal temperature produced by HIFU combined with a 95% high-concentration ethanol in porcine liver tissue were significantly greater than those produced by a 20% low-concentration ethanol, and this phenomenon became more pronounced as the volume of injected ethanol gradually increased. This also proved that injecting a large volume of high-concentration ethanol into porcine liver tissue before HIFU irradiation can effectively enhance the volume of lesions caused by HIFU irradiation on porcine liver tissue.

There were two reasons why ethanol enhanced inertial cavitation in porcine liver tissue. Firstly, ethanol solutions may contain small bubbles (cavitation nuclei) that were activated when exposed to HIFU [38]. The increase in the number of cavitation nuclei reduced the threshold for inertial cavitation [39]. Secondly, ethanol was a volatile substance with a vapor pressure much higher than water. It was well known that an increase in vapor pressure would lower the threshold for inertial cavitation [40]. In addition, ethanol can be mixed with water, and if its volume fraction reaches 90% or more, it cannot be separated from water (this solution was called an azeotropic mixture). The azeotropic mixture had a higher vapor pressure than any pure component, and it should be noted that liver tissue had a high water content.

Ethanol can not only improve the heating of porcine liver tissue by low-power HIFU, but also prevent excessive heating of tissue by high-power HIFU. According to the research results of Mertl *et al.* the boiling point of ethanol-water mixture can increase by up to 4 °C, with the volume fraction of water changing from 5% to 83%. The boiling point of pure ethanol was about 78.5 °C, and the cavitation threshold was relatively low. We expect that the temperature generated by boiling a



20% and a 95% ethanol in porcine liver tissue under HIFU irradiation will be higher than 78.5 °C but still lower than the boiling point of water by 100 °C. Therefore, using ethanol with an evaporative cooling effect can potentially reduce the risk of side effects caused by high-power HIFU irradiation induced water boiling in tissue. The boiling point of 95% concentration ethanol was about 78.3 °C, while the boiling point of 20% concentration ethanol was about 87.1 °C. Under the same HIFU irradiation-power conditions, the same volume of a 95% concentration of ethanol and a 20% concentration of ethanol were injected into porcine liver tissue, respectively. A 95% concentration of ethanol was more prone to the cavitation effect in porcine liver tissue, and its cavitation threshold was lower because it caused lesion volume greater than that caused by a 20% concentration of ethanol. For the same concentration of ethanol, as the volume of injected ethanol gradually increased, the probability of cavitation occurring in porcine liver tissue was higher and the cavitation threshold was also lower.

## Conclusion

This study investigated the combined effects of HIFU with ethanol of varying concentrations and volumes on porcine liver lesion volume and focal temperature. The results demonstrated that this combination therapy decreased the inertial cavitation threshold, leading to an increased volume of porcine liver tissue lesions. Furthermore, lesion volume exhibited a positive correlation with both ethanol concentration and injection volume. These findings suggest that combining HIFU with different ethanol concentrations and volumes can improve the efficacy of tumor ablation therapy. Future studies are warranted to determine whether injecting different ethanol concentrations and volumes into living tissue will yield consistent bio-damage effects.

## Acknowledgment

The authors truly appreciate the anonymous reviewers' helpful remarks and ideas.

## Authors' Contribution

H. Dong conceived and designed the research idea and framework; J. Hu performed the simulations; X. Zou analyzed the experimental data and wrote the manuscript. W. Chen revised the paper. All authors have read and agreed to the published version of the manuscript.

## Ethical Approval

The School of Information Science and Engineering at Changsha Normal University has approved the research and use of necessary resources.

## Funding

This study was funded by the Hunan Provincial Department of Education Key Project (project No. 21A0618), and Changsha Natural Science Foundation Project (grant No.kq2202313).

## Conflict of Interest

None

## References

1. Huber PM, Afzal N, Arya M, Boxler S, Dudderidge T, Emberton M, et al. Focal HIFU therapy for anterior compared to posterior prostate cancer lesions. *World J Urol.* 2021;**39**(4):1115-9. doi: 10.1007/s00345-020-03297-7. PubMed PMID: 32638084. PubMed PMCID: PMC8124043.
2. Cabras P, Auloge P, Bing F, Rao PP, Hoarau S, Dumont E, et al. A new versatile MR-guided high-intensity focused ultrasound (HIFU) device for the treatment of musculoskeletal tumors. *Sci Rep.* 2022;**12**(1):9095. doi: 10.1038/s41598-022-13213-1. PubMed PMID: 35641597. PubMed PMCID: PMC9156664.
3. Zulkifli D, Manan HA, Yahya N, Hamid HA. The Applications of High-Intensity Focused Ultrasound (HIFU) Ablative Therapy in the Treatment of Primary Breast Cancer: A Systematic Review. *Diagnostics (Basel).* 2023;**13**(15):2595. doi: 10.3390/

- diagnostics13152595. PubMed PMID: 37568958. PubMed PMCID: PMC10417478.
4. Dong Z, Zheng H, Zhu Q, Wang Y. Focus prediction of high-intensity focused ultrasound (HIFU) in biological tissues based on magnetic resonance images. *Applied Acoustics*. 2022;**197**:108927. doi: 10.1016/j.apacoust.2022.108927.
  5. Zhou Y. Theoretically Estimating the Acoustic Intensity of High-Intensity Focused Ultrasound (HIFU) Using Infrared Thermography. *IEEE Trans Ultrason Ferroelectr Freq Control*. 2020;**67**(6):1159-65. doi: 10.1109/TUFFC.2020.2965924. PubMed PMID: 31944971.
  6. Mortazavi S, Mokhtari-Dizaji M. Numerical study of high-intensity focused ultrasound (HIFU) in fat reduction. *Skin Res Technol*. 2023;**29**(1):e13280. doi: 10.1111/srt.13280. PubMed PMID: 36704882. PubMed PMCID: PMC10155805.
  7. Huang L, Zhou K, Zhang J, Ma Y, Yang W, Ran L, et al. Efficacy and safety of high-intensity focused ultrasound ablation for hepatocellular carcinoma by changing the acoustic environment: microbubble contrast agent (SonoVue) and transcatheter arterial chemoembolization. *Int J Hyperthermia*. 2019;**36**(1):244-52. doi: 10.1080/02656736.2018.1558290. PubMed PMID: 30668189.
  8. Qiao W, Yu Y, Huang Y, Gao W, Liu Z. Impact of focused ultrasound on the ethanol ablation of VX2 liver tumours in rabbits. *Eur Radiol*. 2020;**30**(11):5862-70. doi: 10.1007/s00330-020-06941-3. PubMed PMID: 32533238.
  9. Yang Z, Zhang Y, Zhang R, Zhang H, Ma J, Chen J, et al. A case-control study of high-intensity focused ultrasound combined with sonographically guided intratumoral ethanol injection in the treatment of uterine fibroids. *J Ultrasound Med*. 2014;**33**(4):657-65. doi: 10.7863/ultra.33.4.657. PubMed PMID: 24658945.
  10. Lang BHH, Woo YC, Chiu KW. Combining high-intensity focused ultrasound (HIFU) ablation with percutaneous ethanol injection (PEI) in the treatment of benign thyroid nodules. *Eur Radiol*. 2021;**31**(4):2384-91. doi: 10.1007/s00330-020-07317-3. PubMed PMID: 32974689.
  11. Zhang T, Sun Z, Lu Z, Yang H, Yan Z, Ji Y. Investigation on the pore structure and adsorption capacity of silica aerogels prepared with different cations. *J Mater Sci*. 2023;**58**(15):6602-17. doi: 10.1007/s10853-023-08455-x.
  12. Tan Y, Ding X, Long H, Ye J, Huang T, Lin Y, et al. Percutaneous ethanol injection enhanced the efficacy of radiofrequency ablation in the treatment of HCC: an insight into the mechanism of ethanol action. *Int J Hyperthermia*. 2021;**38**(1):1394-400. doi: 10.1080/02656736.2021.1977857. PubMed PMID: 34542014.
  13. Yuldashev PV, Karzova MM, Kreider W, Rosnitskiy PB, Sapozhnikov OA, Khokhlova VA. "HIFU Beam:" A Simulator for Predicting Axially Symmetric Nonlinear Acoustic Fields Generated by Focused Transducers in a Layered Medium. *IEEE Trans Ultrason Ferroelectr Freq Control*. 2021;**68**(9):2837-52. doi: 10.1109/TUFFC.2021.3074611. PubMed PMID: 33877971. PubMed PMCID: PMC8486313.
  14. Kagami S, Kanagawa T. Weakly nonlinear propagation of focused ultrasound in bubbly liquids with a thermal effect: Derivation of two cases of Khokhlov-Zabolotskaya-Kuznetsov equations. *Ultrason Sonochem*. 2022;**88**:105911. doi: 10.1016/j.ultrasonch.2022.105911. PubMed PMID: 35810619. PubMed PMCID: PMC9696949.
  15. Zawada T, Bove T. Strongly Focused HIFU Transducers With Simultaneous Optical Observation for Treatment of Skin at 20 MHz. *Ultrasound Med Biol*. 2022;**48**(7):1309-27. doi: 10.1016/j.ultrasmedbio.2022.03.002. PubMed PMID: 35410743.
  16. Dong H, Liu G, Tong X. Influence of temperature-dependent acoustic and thermal parameters and nonlinear harmonics on the prediction of thermal lesion under HIFU ablation. *Math Biosci Eng*. 2021;**18**(2):1340-51. doi: 10.3934/mbe.2021070. PubMed PMID: 33757188.
  17. Mortazavi S, Mokhtari-Dizaji M. Threshold of Linear and Non-Linear Behavior of High Intensity Focused Ultrasound (HIFU) in Skin, Fat, and Muscle Tissue Using Computer Simulation. *Iran J Med Phys*. 2022;**19**:181-8. doi: 10.22038/IJMP.2021.59077.1992.
  18. Qi M, Liu J, Mao Y, Liu X. Temperature rise induced by an annular focused transducer with a wide aperture angle in multi-layer tissue. *Chinese Physics B*. 2018;**27**(1):14301. doi: 10.1088/1674-1056/27/1/014301.
  19. Ge-Pu G, Hui-Dan S, He-Ping D, Qing-Yu M. Noninvasive temperature monitoring for high intensity focused ultrasound therapy based on electrical impedance tomography. *Acta Physica Sinica*. 2017;**66**(16):164301. doi: 10.7498/aps.66.164301.
  20. Zhao P, Wang Y, Tong S, Tao J, Sheng Y. The Effects of Energy on the Relationship between the Acoustic Focal Region and Biological Focal Region during Low-Power Cumulative HIFU Ablation. *Appl*

- Sci.* 2023;**13**(7):4492. doi: 10.3390/app13074492.
21. Zhang Y, Zhang H, Sun T, Pan T, Wang P, Jian X. Numerical simulations of partial elements excitation for hemispherical high-intensity focused ultrasound phased transducer. *Chinese Physics B.* 2021;**30**(7):078704. doi: 10.1088/1674-1056/ac05a2.
  22. Sojahrood AJ, Earl R, Haghi H, Li Q, Porter TM, Kolios MC, Karshafian R. Nonlinear dynamics of acoustic bubbles excited by their pressure-dependent subharmonic resonance frequency: influence of the pressure amplitude, frequency, encapsulation and multiple bubble interactions on oversaturation and enhancement of the subharmonic signal. *Nonlinear Dynamics.* 2021;**103**:429-66. doi: 10.1007/s11071-020-06163-8.
  23. Dong H, Liu G, Peng G. Numerical Simulation of the Effect of Temperature- dependent Acoustic and Thermal Parameters on the Focal Temperature and Thermal Lesion of Biological Tissue Irradiated by HIFU. *Iran J Med Phys.* 2023;**20**:257-65. doi: 10.22038/IJMP.2022.65642.2126.
  24. Cambronero S, Dupré A, Mastier C, Melodelima D. Non-invasive High-Intensity Focused Ultrasound Treatment of Liver Tissues in an In Vivo Porcine Model: Fast, Large and Safe Ablations Using a Toroidal Transducer. *Ultrasound Med Biol.* 2023;**49**(1):212-24. doi: 10.1016/j.ultrasmedbio.2022.08.015 PubMed PMID: 36441030.
  25. Zhao X, Wright A, Goertz DE. An optical and acoustic investigation of microbubble cavitation in small channels under therapeutic ultrasound conditions. *Ultrason Sonochem.* 2023;**93**:106291. doi: 10.1016/j.ulsonch.2023.106291. PubMed PMID: 36640460. PubMed PMCID: PMC9852793.
  26. Horiba T, Ogasawara T, Takahira H. Cavitation inception pressure and bubble cloud formation due to the backscattering of high-intensity focused ultrasound from a laser-induced bubble. *J Acoust Soc Am.* 2020;**147**(2):1207. doi: 10.1121/10.0000649. PubMed PMID: 32113276.
  27. Woodacre JK, Landry TG, Brown JA. Fabrication and Characterization of a 5 mm × 5 mm Aluminum Lens-Based Histotripsy Transducer. *IEEE Trans Ultrason Ferroelectr Freq Control.* 2022;**69**(4):1442-51. doi: 10.1109/TUFFC.2022.3152174. PubMed PMID: 35171768.
  28. He M, Zhong Z, Zeng D, Gong X, Wang Z, Li F. Effects of sub-atmospheric pressure and dissolved oxygen concentration on lesions generated in ex vivo tissues by high intensity focused ultrasound. *Biomed Eng Online.* 2021;**20**(1):91. doi: 10.1186/s12938-021-00926-z. PubMed PMID: 34526014. PubMed PMCID: PMC8442382.
  29. Ponomarchuk EM, Hunter C, Song M, Khokhlova VA, Sapozhnikov OA, Yuldashev PV, Khokhlova TD. Mechanical damage thresholds for hematomas near gas-containing bodies in pulsed HIFU fields. *Phys Med Biol.* 2022;**67**(21):215007. doi: 10.1088/1361-6560/ac96c7. PubMed PMID: 36179703. PubMed PMCID: PMC9645587.
  30. Karunakaran CP, Burgess MT, Rao MB, Holland CK, Mast TD. Effect of Overpressure on Acoustic Emissions and Treated Tissue Histology in ex Vivo Bulk Ultrasound Ablation. *Ultrasound Med Biol.* 2021;**47**(8):2360-76. doi: 10.1016/j.ultrasmedbio.2021.04.006. PubMed PMID: 34023187. PubMed PMCID: PMC8243850.
  31. Khokhlova VA, Rosnitskiy PB, Tsysar SA, Buravkov SV, Ponomarchuk EM, Sapozhnikov OA, et al. Initial Assessment of Boiling Histotripsy for Mechanical Ablation of Ex Vivo Human Prostate Tissue. *Ultrasound Med Biol.* 2023;**49**(1):62-71. doi: 10.1016/j.ultrasmedbio.2022.07.014 PubMed PMID: 36207225. PubMed PMCID: PMC9712256.
  32. Bar-Zion A, Nourmahnad A, Mittelstein DR, Shivaie S, Yoo S, Buss MT, et al. Acoustically triggered mechanotherapy using genetically encoded gas vesicles. *Nat Nanotechnol.* 2021;**16**(12):1403-12. doi: 10.1038/s41565-021-00971-8. PubMed PMID: 34580468.
  33. Zhao P, Wang Y, Wu Y, Hu X, Shen H, Tong S, Tao J. Formation process of thermal damage in a target area of high intensity focused ultrasound and effectiveness analysis of B-ultrasound real-time monitoring. *Acta Acustica.* 2022;**6**(41):1-8. doi: 10.1051/aacus/2022036.
  34. Senegačnik M, Kunimoto K, Yamaguchi S, Kimura K, Sakka T, Gregorčič P. Dynamics of laser-induced cavitation bubble during expansion over sharp-edge geometry submerged in liquid - an inside view by diffuse illumination. *Ultrason Sonochem.* 2021;**73**:105460. doi: 10.1016/j.ulsonch.2021.105460. PubMed PMID: 33774586. PubMed PMCID: PMC8027904.
  35. Reuter F, Ohi CD. Supersonic needle-jet generation with single cavitation bubbles. *Applied Physics Letters.* 2021;**118**(13):134103. doi: 10.1063/5.0045705.
  36. Hoang NH, Murad HY, Ratnayaka SH, Chen C, Khismatullin DB. Synergistic ablation of liver tissue and liver cancer cells with high-intensity focused ultrasound and ethanol. *Ultrasound Med Biol.* 2014;**40**(8):1869-81. doi: 10.1016/j.ultrasmed-

- bio.2014.02.026. PubMed PMID: 24798386.
37. Fischer A, Korkusuz H, Vorländer C. Effectiveness of High-intensity Focused Ultrasound (HIFU) Therapy of Solid and Complex Benign Thyroid Nodules - A Long-term Follow up Two-center Study. *Exp Clin Endocrinol Diabetes*. 2022;**130**(6):374-80. doi: 10.1055/a-1719-4441. PubMed PMID: 35008118.
38. Brezhneva N, Dezhkunov NV, Ulasevich SA, Skorb EV. Characterization of transient cavitation activity during sonochemical modification of magnesium particles. *Ultrason Sonochem*. 2021;**70**:105315. doi: 10.1016/j.ultsonch.2020.105315. PubMed PMID: 32906064. PubMed PMCID: PMC7786532.
39. Wang C, Li Z, Bai J. Bubble-assisted HIFU ablation enabled by calcium peroxide. *J Mater Chem B*. 2022;**10**(23):4442-51. doi: 10.1039/d2tb00587e. PubMed PMID: 35593261.
40. Ge M, Petkovšek M, Zhang G, Jacobs D, Coutier-Delgosha O. Cavitation dynamics and thermodynamic effects at elevated temperatures in a small Venturi channel. *International Journal of Heat and Mass Transfer*. 2021;**170**:120970. doi: 10.1016/j.ijheatmasstransfer.2021.120970.